

## Microscopic model for a class of mixed-spin quantum antiferromagnets

J. V. Alvarez,<sup>1</sup> Roser Valentí,<sup>1</sup> and A. Zheludev<sup>2,\*</sup>

<sup>1</sup>Fakultät 7, Theoretische Physik, University of the Saarland, 66041 Saarbrücken, Germany

<sup>2</sup>Solid State Division, Oak Ridge National Laboratory, Oak Ridge, Tennessee 37831-6393

(Received 12 February 2002; published 26 April 2002)

We propose a microscopic model that describes the magnetic behavior of the mixed-spin quantum systems  $R_2\text{BaNiO}_5$  ( $R$ =magnetic rare earth). An evaluation of the properties of this model by quantum Monte Carlo simulations shows remarkable good agreement with the experimental data, and provides insight into the physics of mixed-spin quantum magnets.

DOI: 10.1103/PhysRevB.65.184417

PACS number(s): 75.10.Jm, 75.25.+z, 75.50.Ee

Low-dimensional (low- $D$ ) quantum magnetism remains at the forefront of condensed-matter research for almost two decades. This is primarily because this field deals with *simple* models of magnetism that demonstrate a broad spectrum of *complex* quantum-mechanical phenomena of a general and fundamental nature. The simplicity of the Hamiltonians involved, as well as the low dimensionality, often allow accurate theoretical and numerical treatments. On the other hand, the discovery of real low- $D$  materials allows experimental studies for direct comparison with theory on the quantitative level. A particular area of great recent interest is the coexistence of “quantum” and “classical” properties in systems composed of weakly coupled quantum spin chains. One good example is the interplay between continuum and spin-wave dynamics in gapless quasi-one-dimensional (quasi-1D) Heisenberg systems such as  $\text{KCuF}_3$  (Ref. 1) and  $\text{BaCu}_2\text{Si}_2\text{O}_7$ .<sup>2</sup> At the focus of the present work is a more complex phenomenon: the seemingly paradoxical coexistence of 3D magnetic long-range order and 1D quantum gap excitations in rare-earth nickelates with the general formula  $R_2\text{BaNiO}_5$  ( $R$ =magnetic rare earth).<sup>3,4</sup>

$R_2\text{BaNiO}_5$  species have two types of spin carriers.  $S=1$   $\text{Ni}^{2+}$  ions form distinct antiferromagnetic chains running along the  $a$  axis of the crystal structure. If these chains were perfectly isolated, they would be a classic example of a Haldane antiferromagnet with no long-range order even at  $T=0$  and a gap in the magnetic excitation spectrum.<sup>5</sup> Long-range ordering that occurs in  $R_2\text{BaNiO}_5$  at low temperatures is driven by the magnetic  $s=\frac{1}{2}$   $R^{3+}$  ions, positioned in-between the chains. 3D magnetic order involves *both*  $R^{3+}$  and  $\text{Ni}^{2+}$  spins. What is particularly interesting, though, is that Haldane-gap excitations associated with the Ni chains *persist* in the ordered state and *coexist* with conventional order-parameter excitations (spin waves). By now, a wealth of experimental data on several  $R_2\text{BaNiO}_5$  compounds has been accumulated.<sup>3,4,6</sup> Most theoretical work, however, was based on a simple mean-field (MF) (Ref. 4) or random phase approximation (RPA) (Ref. 7) treatment of the interactions between Ni-chain and-rare earth subsystems. The existing numerical studies were aimed at calculating the “bare” properties of the Ni chains, needed to complete the MF/RPA equations.<sup>8</sup> While the MF/RPA approach turned out to be an extremely useful tool in understanding the basic physics involved, it has numerous intrinsic limitations, particularly for dilute  $(R_{1-x}Y_x)_2\text{BaNiO}_5$  systems,<sup>9</sup> or in the case of strong

Ni- $R$  coupling. In the present work we abolish the MF/RPA framework and construct a *microscopic* model for  $R_2\text{BaNiO}_5$  compounds. We then employ this model in a systematic first-principles numerical study of these interesting materials.

In order to construct the microscopic model we will use the available experimental results to design an appropriate description for the magnetic ions and interactions in the system: (i) A good understanding of the Ni subsystem can be drawn from the known properties of  $\text{Y}_2\text{BaNiO}_5$ , a material where the magnetic rare earths have been replaced by non-magnetic  $\text{Y}^{3+}$ . The yttrium nickelate is an almost perfect physical realization of a Haldane gap antiferromagnet. Neutron-scattering data<sup>10</sup> show a large gap of  $\Delta\sim 10$  meV and well-characterized Haldane excitations. This suggests that the intrachain Ni-Ni exchange coupling in the chains running along the  $a$  axis has to be  $J\sim 25$  meV. Furthermore, there is no evidence of 3D long-range order even at the lowest temperatures. Any residual *direct* coupling between the chains, both in  $b$  and  $c$  directions, is smaller than the critical value necessary to establish antiferromagnetic order at low enough temperatures.<sup>11,12</sup> This critical value depends quadratically on the gap, and it is expected to be large in this family of nickelates due to the magnitude of the gap. Therefore, we will consider the *direct* Ni-Ni interchain coupling irrelevant for a physical description of the material.

(ii) When Y, located between the chains, is completely substituted by a magnetic rare earth  $R$ , the system orders antiferromagnetically. The Néel temperature is typically smaller than the gap energy. For example, in the case  $R=\text{Nd}$ ,  $T_N=48$  K and  $\Delta\sim 11$  meV ( $\sim 127$  K).<sup>13</sup> In the *paramagnetic* phase ( $T>T_N$ ), the Ni-chain excitations in  $R_2\text{BaNiO}_5$  are virtually indistinguishable from those in the yttrium compound at the same temperature, implying that very little should change in the model of the  $S=1$  chains while the ordering should be driven by some kind of exchange Ni- $R$  that induces an *indirect* coupling between the chains.

(iii) In the magnetically ordered phase, the staggered magnetization of the Ni sublattice has as  $T\rightarrow 0$  saturation values of  $(1.0-1.6)\mu_B$  per ion in all the  $R_2\text{BaNiO}_5$  studied to date.<sup>4,14,15</sup> These values are clearly smaller than the classical result  $2\mu_B$ . This observation signals that the model describing these compounds has to properly retain the quantum fluctuations in the ordered phase.

(iv) Unlike Ni- $R$  interactions, that are vital in order to induce a static magnetization on the Ni sites below  $T_N$ , direct  $R$ - $R$  magnetic coupling can be disregarded in our model. Indeed, the ordering temperatures in  $R_2\text{BaNiO}_5$  compounds are typically several tens of K. The direct coupling strength between rare earths in insulators is much weaker, usually of the order of 1 K. This is due to the fact that in rare earth species the magnetic  $f$  electrons are strongly localized, which prevents efficient superexchange coupling.<sup>16</sup> Unlike the case of  $\text{Y}_{2-x}\text{Ca}_x\text{BaNiO}_5$ ,<sup>17-19</sup> where doping with Ca introduces hole carriers in the Ni chains, this localized nature of  $f$ -electrons in the rare-earth keeps the  $S=1$  chains free from charge carriers.<sup>20</sup>

(v) In the crystal structure of  $R_2\text{BaNiO}_5$ , the site-symmetry for  $R^{3+}$  is very low. As a result, for each rare-earth ion the degeneracy of its magnetic multiplet is lifted by crystal-field effects. To investigate the low-energy part of the spectrum we only need to consider the lowest-energy orbital levels. In the case of the rare earth being a Kramers ion with half-integer total angular momentum,<sup>16</sup> we shall model the magnetic rare earths by effective  $s=\frac{1}{2}$  (pseudo)spins. In order to decide about the type of coupling between the Ni and  $R$  sublattices, we rely on the experimental observation of the absence of dispersion in the crystal field excitations associated with  $R^{3+}$  ions.<sup>7</sup> This fact suggests that the coupling between the  $R$  and Ni sublattices is very anisotropic and can be approximated by an Ising-type term in the Hamiltonian.

With all the ingredients above, we now propose the Hamiltonian

$$H = J \sum_{ij} \mathbf{S}_{i,2j} \mathbf{S}_{i+1,2j} + J_c \sum_{ij} S_{i,2j}^z (s_{i,2j-1}^z + s_{i,2j+1}^z),$$

with  $J$  and  $J_c$  both positive. The first term in  $H$  is a  $S=1$  Heisenberg model along the Ni chains, the second is an Ising-like coupling with strength  $J_c$  between the  $S=1$  Ni ions and the  $s=\frac{1}{2}$  magnetic moment in the rare earth. The index  $i$  runs along the chain direction and  $j$  in the direction perpendicular to the chains. A sketch of the model is shown in Fig. 1. When  $J_c=0$ ,  $H$  should reproduce the physics of the  $\text{Y}_2\text{BaNiO}_5$ , i.e., basically independent  $S=1$  chains.

We have studied this model numerically with the quantum Monte Carlo (QMC) method using a quantum cluster algorithm, the loop algorithm.<sup>21</sup> This method allows for an efficient sampling of the configuration space giving a specific prescription of how to perform global updates in quantum systems. Such updates involve clusters of spins with a size of the correlation length. The Hamiltonian we studied is not frustrated, and does not show the sign problem. All the Boltzmann weights can be taken positive after the conventional rotation around the  $z$  axis of all the spins in one of the two sublattices of the  $S=1$  system. The difficulty in reaching extremely low temperatures is a drawback of the QMC method when one is interested in characterizing exotic ground states, mostly near quantum critical points or strongly frustrated systems. None of these cases affects our calculations, since our main goal is to compare with experimental results at temperatures, as we will see, perfectly accessible for the QMC method. We have measured various magnitudes

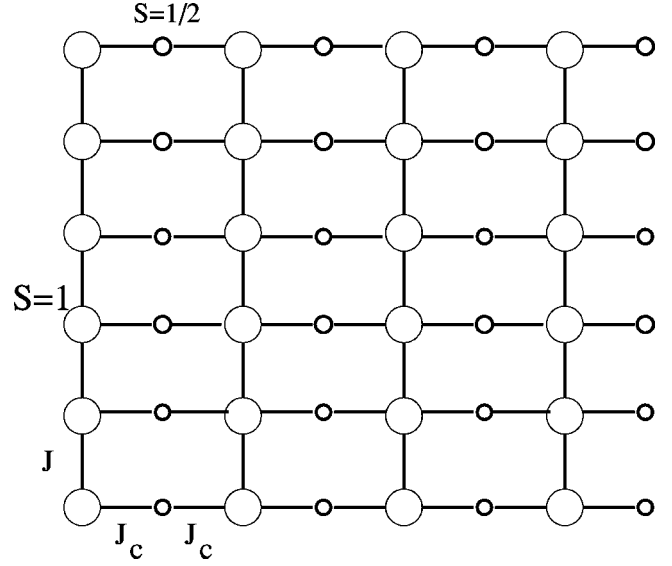


FIG. 1. Microscopic model for  $R_2\text{BaNiO}_5$ . The large circles denote  $S=1$  Ni spins, and the small circles denote the  $s=\frac{1}{2}$   $R$  spins.  $J$  and  $J_c$  are the Ni-Ni and the Ni- $R$  exchange couplings respectively.

that can be directly compared with the available experimental data and which, in some cases, are not accessible for other approaches like the MF/RPA approximation<sup>4,7</sup> or the zero temperature density-matrix renormalization-group (DMRG) calculations.<sup>8</sup> These magnitudes are (i) magnetizations in both sublattices, (ii) Néel temperatures, and (iii) correlation lengths and gaps in both subsystems.

Before discussing the results, we present a brief technical description of the numerical work and data treatment. QMC simulations are performed in finite lattices; therefore, an exhaustive finite size analysis of the results is necessary to compare with real experiments. We used periodic boundary conditions. The magnetization ( $M$ ) was computed by directly measuring  $|M|$  in order to avoid the averaging between configurations around the two ground states of the model in the ordered phase, and by using the relation  $M = \lim_{L \rightarrow \infty} |M|$ . We considered for this extrapolation  $L \times L$  lattices of size  $L=8, 16, 24, 32, 48$ , and  $64$  spins. The Néel temperature was then determined by using the Binder parameter,<sup>22</sup> which is the fourth cumulant of the order parameter distribution. At  $T_N$  this cumulant is independent of the size of the system, apart from subdominant corrections. We have observed that for values of  $J_c$  smaller than  $\sim 0.1J$  these corrections are due to the anisotropy in the scaling (i.e., different numbers of spins in the  $a$  and  $c$  directions). We have checked this point by studying systems with different sizes  $L_a=32$  and  $48$  spins and  $L_c=24, 32$ , and  $48$  spins. For values of  $J_c \sim 0.3$  and the precision needed for comparison with the experiment,  $T_N$  can be computed by extrapolation from isotropic lattices. The statistical error bars are always smaller than the symbol sizes in all the figures presented. We measured all the magnitudes in  $10^5$  Monte Carlo steps after thermalization. We have used units  $\mu_B = k_B = \hbar = 1$ .

The staggered magnetizations obtained from the QMC computations for both the nickel ( $M_{\text{Ni}}$ ) and rare-earth ( $M_R$ )

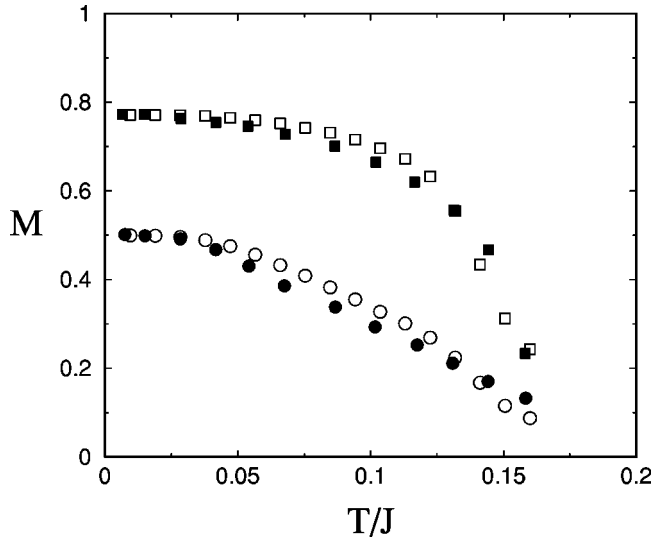


FIG. 2.  $M_{\text{Ni}}$  (squares) and  $M_{\text{R}}$  (circles) vs  $T$ . Open symbols are the results obtained with the model Hamiltonian for  $J_c = 0.31J$ , and filled symbols are the experimental data. Both magnetizations are given in units of  $\mu_B$ , and have been rescaled with respect to the saturation values 1 and 0.5, respectively.

sublattices are in good agreement with the experimental results for  $\text{Nd}_2\text{BaNiO}_5$  (Ref. 4) for a suitable choice of the model parameters in the Hamiltonian. For instance, for a value of the transverse coupling  $J_c = 0.31J$ , we have that  $M_{\text{Ni}}(T \rightarrow 0) = 0.79$  that corresponds to the value  $1.6\mu_B$  observed experimentally. The Néel temperature for this value of  $J_c$  is  $T_N = 0.163J$ . We can take the gap in a single  $S = 1$  chain,  $\Delta = 0.410J$ , and compute the ratio between the two main energy scales in the system  $r = \Delta/T_N$ . We observe that  $r$  is very similar in the material ( $r = 2.59$ ) and in the model ( $r = 2.51$ ). In Fig. 2 we present the temperature dependence of the staggered magnetizations in the  $S = 1$  (open squares) and  $s = \frac{1}{2}$  (open circles) sublattices,  $M_{\text{Ni}}$  and  $M_{\text{R}}$ , respectively, for the selected value of  $J_c$  obtained from the QMC simulations. The magnetization results have been rescaled with respect to the maximum saturation values, i.e., 1 for the  $S = 1$  system and 0.5 for the  $s = \frac{1}{2}$  system. The results can be compared with the experimental magnetic moment in the Ni (filled squares) and Nd systems (filled circles).<sup>4</sup> Note the good agreement between the theoretical and experimental results at low temperatures. We also observe that the staggered magnetization in the  $S = 1$  sublattice is nearly temperature independent for  $T \leq T_N/2$ . At  $T = 40$  K, the  $\text{Nd}_2\text{NiBaO}_5$  undergoes a magnetic structural transition,<sup>23</sup> and therefore we expect only qualitative agreement with our model at temperatures near  $T_N$ .

Both sublattices behave qualitatively differently in the ordered phase. While in the Ni sublattice the reduction of the staggered magnetization by purely quantum fluctuations is important, the R sublattice is fully saturated to the classical value  $M_{\text{R}} = 0.5$  at  $T = 0$ .

In order to understand the origin of the ordered phase of this quantum model we have studied the relation between the magnetizations in both sublattices for different values of  $J_c$ . In Fig. 3(a) we show a plot of the QMC results at  $T < T_N$  for

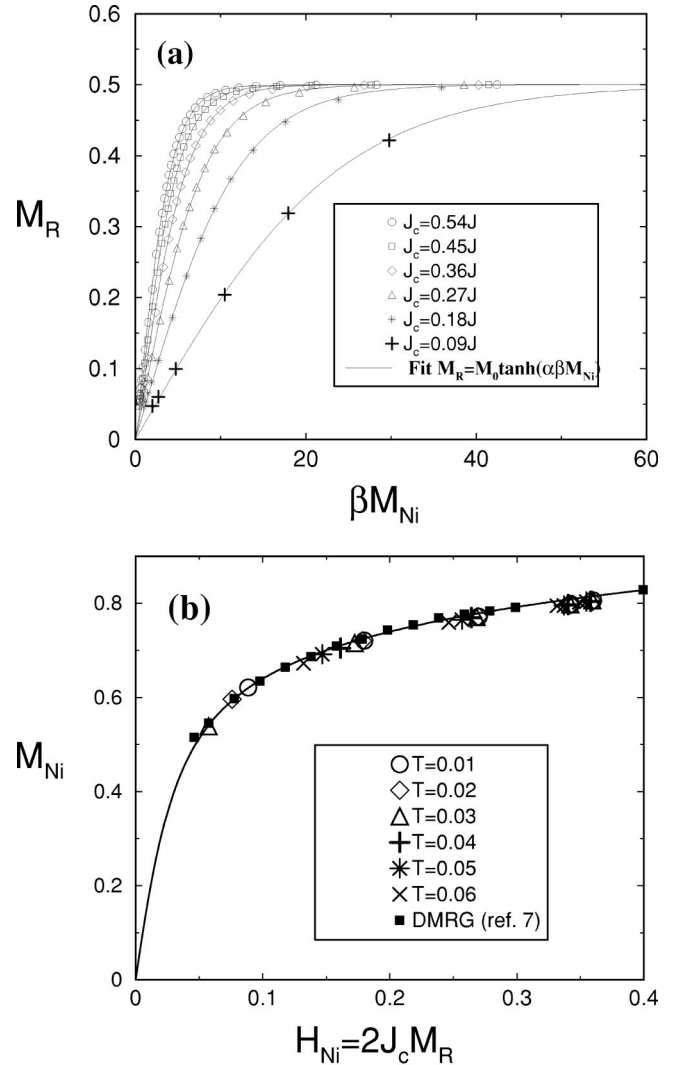


FIG. 3. QMC results for (a)  $M_{\text{R}}$  vs  $M_{\text{Ni}}$  for various values of the coupling constant  $J_c$ . The solid lines correspond to the function Eq. (1). (b)  $M_{\text{Ni}}$  vs the “effective” field on the Ni subsystem induced by  $M_{\text{R}}$  (Ref. 4) for various  $T$  values. The squares correspond to the DMRG results (Ref. 8) at  $T = 0$ .

$M_{\text{R}}$  as a function of  $M_{\text{Ni}}$  for various values of  $J_c$ . We observe that the behavior of the magnetizations is well reproduced by the function

$$M_{\text{R}} = M_0 \tanh(\alpha \beta M_{\text{Ni}}), \quad (1)$$

where  $\beta = 1/k_B T$ ,  $M_0$  is the effective moment of the rare-earth ion, and  $\alpha$  is a linear function of  $J_c$  in the range  $0.09 < J_c < 0.5J$  as observed from our QMC results. Equation (1) can be obtained by a mean-field approach, as shown by Zheludev *et al.*<sup>4</sup> These authors considered that the behavior of the  $\text{R}_2\text{BaNiO}_5$  compounds in the ordered phase could be described in terms of a  $S = 1$  chain of Ni ions in a staggered magnetic field induced by the  $s = \frac{1}{2}$  magnetic rare-earth ions and, reciprocally, the otherwise free spins  $s = \frac{1}{2}$  see the mean field produced by the neighboring  $S = 1$  chains.

The excellent agreement between this mean-field approach and our QMC results indicates that our microscopic

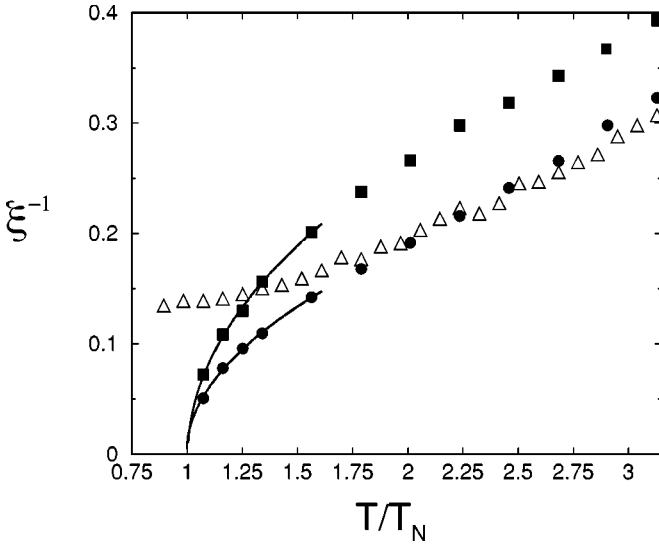


FIG. 4. Inverse correlation length vs temperature for the Ni-chain subsystem (circles), the  $R$  subsystem along  $a$  (squares), and for a single  $S=1$  chain (triangles). Solid lines correspond to the law  $\xi^{-1} \sim (T - T_N)^{1/2}$ . At higher  $T$ , the Ni subsystem behaves like a Haldane  $S=1$  chain.

model also fulfills the property of viewing the effect of the staggered magnetization on the rare-earth ions as an effective magnetic field on the Ni subsystem, and vice versa. In Fig. 3(b) we show the relation between  $M_{\text{Ni}}$  and the staggered magnetic field induced by  $M_R$  obtained by our QMC calculations for various  $T$  values. The extrapolation  $T \rightarrow 0$  reproduces the DMRG results for one  $S=1$  chain in a staggered magnetic field at  $T=0$  obtained by Yu *et al.*<sup>8</sup> Since the  $R$  sublattice is fully polarized at  $T=0$  no rescaling is necessary to compare our data with the DMRG results. The quality of the fits in Fig. 3(a) and the data collapse in Fig. 3(b) suggests a technical procedure to extrapolate QMC data down to zero temperature. This procedure is obvious for magnetizations but could be extended for other thermodynamic magnitudes for Hamiltonians similar to the one proposed here.

In the context of the effective field interpretation, an analysis of the temperature dependence of  $M_R$  obtained with our QMC simulations indicates that, though  $M_R$  saturates to the classical value at  $T=0$  (see Fig. 2), as expected if we consider this subsystem as a sublattice of free spins in the presence of an external field, this behavior cannot be reproduced by a purely classical mean-field model in the  $R$  sublattice, namely, the mean field just proportional to the magnetization in the  $R$  sublattice and independent of the Ni magnetization. This fact signals that quantum fluctuations in the Ni sublattice are essential to describe the magnetization in the  $R$  sublattice.

We now discuss the spatial spin-spin correlations in the paramagnetic phase. In Fig. 4 we plot the inverse of the correlation length  $\xi^{-1}$  along the Ni chains (circles) and along the  $R$  chains parallel to the Ni chains (squares) for  $T < \Delta/2$ . For comparison, we present  $\xi^{-1}$  in a single  $S=1$  spin chain (triangles). In this range of temperatures it is well known that the correlation length in the  $S=1$  chain is  $\xi = \hbar c / \Delta$ , where  $c$

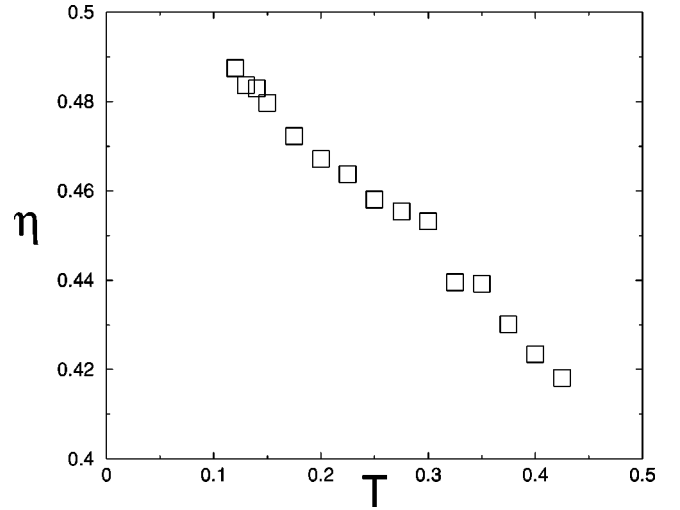


FIG. 5. Temperature dependence of the fitting parameter  $\eta(T)$  in Eq. (2) for the Ni subsystem.

is the spin-excitation velocity. The correlation length is computed in all the cases by fitting the  $z$ -component of the spin-spin correlation function to the law<sup>24</sup>

$$|\langle S_0^z S_l^z \rangle| = A \exp\left(\frac{-l}{\xi}\right) l^{-\eta} \quad (2)$$

( $A$  and  $\eta$  are fitting parameters) directly in a lattice of  $64 \times 64$  spins and for  $J_c = 0.18$  to keep  $T_N$  and  $\Delta$  well separated in energy. Near  $T_N$ , the critical modes become gapless and we observe how the gap closes in both subsystems following a law  $\xi^{-1} = K(T - T_N)^{1/2}$ .  $K$  is the only free parameter in the fit presented in Fig. 4 by the solid line, since  $T_N$  is computed independently. As the temperature increases, the correlation length in the Ni subsystem approaches the correlation length of a single chain.

The behavior of  $\eta$  is completely different in both sublattices. While in the  $R$  sublattice the correlation function  $\langle S_0^z S_l^z \rangle$  can be fitted with  $\eta=0$  for all the temperatures showed in Fig. 4, in the Ni sublattice  $\eta$  approaches the value 0.5 in Eq. (2) as the temperature is reduced in the paramagnetic phase. We have analyzed this behavior and observed that the temperature dependence of  $\eta(T)$  in the spin-spin correlation function Eq. (2) is very similar to that of  $\eta$  in a single chain in which Eq. (2) shows a slow crossover from  $\eta = \frac{1}{2}$  at  $T=0$ , more precisely  $\langle S_0^z S_l^z \rangle$  is then described by the modified Bessel function  $K_0$ ,<sup>25</sup> to  $\eta=0$  when  $T > \Delta$ .<sup>26</sup> The temperature dependence of  $\eta(T)$  is shown in Fig. 5.

The picture arising from the study of the spin-spin correlation functions is that the modes becoming gapless at  $T_N$  can be described at a mean-field level. Moreover, since both the value of the correlation length and the power-law corrections to the exponential behavior are very similar for the Ni subsystem and for an independent  $S=1$  chain, we can conclude that the modes remaining gapped in the system are very much like the conventional Haldane excitations.

In summary, we have shown that QMC calculations based

on the proposed microscopic model are able to reproduce the observed behavior of  $R_2\text{BaNiO}_5$  mixed-spin quantum anti-ferromagnets remarkably well. They provide a solid numerical basis for the MF/RPA model, and make additional predictions regarding the magnetic nature of both spin species that go beyond the simplistic picture of a MF/RPA model. We hope that the proposed approach will be particularly useful in the study of dilute  $(R_x\text{Y}_{1-x})_2\text{BaNiO}_5$  compounds in

the limit of small  $x$ , where the MF model becomes totally inadequate.

It is a pleasure for us to acknowledge discussions with C. Gros, F. Mila, and H. Rieger. Oak Ridge National Laboratory is managed by UT-Battelle, LLC for the U.S. Department of Energy under Contract No. DE-AC05-00OR22725. R.V. acknowledges financial support from the Deutsche Forschungsgemeinschaft.

\*Previous address: Physics Department, Brookhaven National Laboratory, Upton, New York 11973-5000.

- <sup>1</sup>D.A. Tennant, S.E. Nagler, D. Welz, G. Shirane, and K. Yamada, Phys. Rev. B **52**, 13 381 (1995); B. Lake, D.A. Tennant, and S. E. Nagler, Phys. Rev. Lett. **85**, 832 (2000).
- <sup>2</sup>A. Zheludev, M. Kenzelmann, S. Raymond, E. Ressouche, T. Masuda, K. Kakurai, S. Maslov, I. Tsukada, K. Uchinokura, and A. Wildes, Phys. Rev. Lett. **85**, 4799 (2000).
- <sup>3</sup>E. García-Matres, J.L. García-Munoz, J.L. Martínez, and J. Rodríguez-Carvajal, J. Magn. Magn. Mater. **149**, 363 (1995).
- <sup>4</sup>A. Zheludev, E. Ressouche, S. Maslov, T. Yokoo, S. Raymond, and J. Akimitsu, Phys. Rev. Lett. **80**, 3630 (1998).
- <sup>5</sup>F.D.M. Haldane, Phys. Rev. Lett. **50**, 1153 (1983).
- <sup>6</sup>S. Raymond, T. Yokoo, A. Zheludev, S. E. Nagler, A. Wildes, and J. Akimitsu, Phys. Rev. Lett. **82**, 2382 (1999).
- <sup>7</sup>A. Zheludev, S. Maslov, T. Yokoo, S. Raymond, S.E. Nagler, and J. Akimitsu, J. Phys.: Condens. Matter **13**, R525 (2001).
- <sup>8</sup>J. Lou, X. Dai, S. Qin, Z. Su, and L. Yu, Phys. Rev. B **60**, 4357 (1999).
- <sup>9</sup>T. Yokoo, S. Raymond, A. Zheludev, S. Maslov, E. Ressouche, I. Zaliznyak, R. Erwin, M. Nakamura, and J. Akimitsu, Phys. Rev. B **58**, 14 424 (1998).
- <sup>10</sup>J. Darriet and L. P. Regnault, Solid State Commun. **86**, 409 (1993); T. Yokoo, T. Sakaguchi, K. Kakurai, and J. Akimitsu, J. Phys. Soc. Jpn. **64**, 3651 (1995); G. Xu, J.F. DiTusa, T. Ito, K. Oka, H. Takagi, C. Broholm, and G. Aeppli, Phys. Rev. B **54**, R6827 (1996).
- <sup>11</sup>I. Affleck, Phys. Rev. Lett. **62**, 474 (1989).
- <sup>12</sup>T. Sakai and M. Takahashi, Phys. Rev. B **42**, 4537 (1990).
- <sup>13</sup>A. Zheludev, J.M. Tranquada, T. Vogt, and D.J. Buttrey, Phys. Rev. B **54**, 7210 (1996).
- <sup>14</sup>J.A. Alonso, J. Amador, J.L. Martínez, I. Rasines, J. Rodríguez-Carvajal, and R. Saez-Puche, Solid State Commun. **76**, 467 (1990).
- <sup>15</sup>E. García-Matres, J.L. Martínez, J. Rodríguez-Carvajal, and A. Salinas-Sánchez, Solid State Commun. **85**, 553 (1993).
- <sup>16</sup>For a review, see *Optical Spectra of Transparent Rare Earth Compounds*, edited by S. Hufner (Academic Press, London, 1978).
- <sup>17</sup>J.F. DiTusa, S-W. Cheong, J.-H. Park, G. Aeppli, G. Broholm, and C.T. Chen, Phys. Rev. Lett. **73**, 1857 (1994).
- <sup>18</sup>E. Dagotto, J. Riera, A. Sandvik and A. Moreo, Phys. Rev. Lett. **76**, 1731 (1996).
- <sup>19</sup>C.D. Batista, A. A. Aligia, and J. Eroles, Europhys. Lett. **43**, 71 (1998).
- <sup>20</sup>S. Maslov and A. Zheludev, Phys. Rev. Lett. **80**, 5786 (1998).
- <sup>21</sup>H.G. Evertz, G. Lana, and M. Marcu, Phys. Rev. Lett. **70**, 875 (1993).
- <sup>22</sup>*Monte Carlo Simulations in Statistical Physics*, edited by D.P. Landau and K. Binder (Cambridge University Press, Cambridge, 2000).
- <sup>23</sup>E. García-Matres, J.L. Martínez, and J. Rodríguez-Carvajal, Physica (Amsterdam) **234-236B**, 567 (1997).
- <sup>24</sup>S. R. White and D.A. Huse, Phys. Rev. B **48**, 3844 (1993).
- <sup>25</sup>E.S. Sorensen and I. Affleck, Phys. Rev. B **51**, 16 615 (1995).
- <sup>26</sup>Y.J. Kim and R.J. Birgeneau, Phys. Rev. B **62**, 6378 (2000).